2007. 02

Master's Thesis

Joining characteristics of Sn-3.5Ag solder joint of induction heating by the material property of pad

Graduate School of Chosun University

Department of Naval Architecture and Ocean Engineering

JUN - KI CHOI

Joining characteristics of Sn-3.5Ag solder joint of induction heating by the material property of pad

패드 물성치에 따른 유도가열 Sn-3.5Ag 솔더 접합부의 접합 특성에 관한 연구

February 2007

Graduate School of Chosun University

Department of Naval Architecture and Ocean Engineering

JUN - KI CHOI

Joining characteristics of Sn-3.5Ag solder joint of induction heating by the material property of pad

Advisor : Professor Han-Sur Bang

A Thesis submitted for the degree of
Master of Engineering

October 2006

Graduate School of Chosun University

Department of Naval Architecture and
Ocean Engineering

JUN - KI CHOI

Contents

List of Figures

List of Tables

초 록

Pad 물성치에 따른 유도가열 *Sn-3.5Ag* 솔더 접합부의 접합 특성에 관한 연구

최 준 기
지도 교수 : 방 한 서
조선대학교 일반 대학원
선박해양공학과

현재 전자·정보통신산업의 급속한 발달에 따라서 표면실장기술은 더욱 고집적화와 고신뢰성 확보를 요구하고 있으며, 전자 부품의 접성도 혹은 단일 전자칩의 I/O 밀도가 부단히 증가되고 있다. 특히 BGA(Ball Grid Array), CSP(Chip Scale Package), FC(Flip Chip) 등의 고밀도 Area Array 패키지는 현재 고주파 통신기기, Micro Electronic Mechanical System, 바이오센서 등의 영역에 많이 사용되고 있다. 기존 솔더링 공정 기술은 이러한 고밀도 실장 적용에 어려움이 있으며, 높은 융점의 무연 솔더 접합 시 기판과 전자부품에 열영향을 주어 부품의 변형 및 파손의 우려가 있다. 이에 전자 산업에 적용이 가능하고 낮은 가격과 높은 신뢰성을 보장하는 새로운 솔더링 공정 기술이 요구된다.

고주파 유도가열은 금속합금의 용융, 담금질, 풀림, 브레이징, 단조 등의 분야에서 사용되어지고 있으며, 솔더링에 응용시 반도체 및 기판의 열영향을 최소화 하고 국부적 가속 가열 실현을 통해 접합부 계면 금속 반응을 제어할 수 있는 이점을 지니고 있다. 본 연구에서는 새로운 솔더링 기술로서 고주파 유도가열을 이용하여 대표적 무연 솔더 합금인 Sn-3.5Ag 솔더 범프의 형성과 그 접합 특성을 평가하고 열전도 해석을 통해 유도가열에 의한 무연 솔더링의 신뢰성을 해석하고, 고주파 유도가열의 솔더링에의 적용 가능성을 확인하고자 하였다.

본 실험에서는 Sn-3.5Ag 솔더볼을 FR4 기판의 도금물질(Au/Ni/Cu, Au/Cu, Ni/Cu,

Cu)을 달리하여 유도가열에 의해 솔더 범핑을 실시하였다. 여기서 고주파 유도가열 장치의 주파수는 300㎑로 고정하고 전류와 가열시간을 조절하여 솔더 범프를 형성시켰으며, 솔더링 중 적외선 온도 측정기를 이용하여 솔더 범프의 발열량을 측정하고 초기조건을 선정하였다. 선정된 초기조건을 이용하여 유도가열에 의해 솔더 범프를 형성하고 전단강도, 계면조직 및 금속간 화합물 두께에 대해 분석하였으며, 유도가열과 열풍리플로 두 공정을 이용하여 각각의 조건에서 솔더 범프를 형성한 후 시효시간에 따른 계면조직 변화를 비교 분석하였다. 또한 유한요소법에 의한 2차원 정상 열전도 해석을 통해 솔더 범프의 온도구배 분포를 분석하여 실험 결과와 비교하였다.

초기조건 선정 실험 결과, 유도가열에 의한 솔더범프의 형성은 전류와 시간이 주요 변수이며, 전해도금물질의 열전도도에 따라 발열량에서 차이를 보여 접합시간에 영향을 미침을 알 수 있었다.

솔더 범프 내에는 다양한 금속간 화합물이 존재하였고, 금속간 화합물은 유도가열시간 및 가열온도, 시효시간에 의해 좌우되었다. 금속간 화합물은 대체로 가열시간과 시효시간이 증가함에 따라 증가함을 볼 수 있었다.

2차원 정상 열전도 해석 결과 접합계면의 양 끝단에서 큰 온도변화를 보였으며, 그 주위로 응력이 많이 분포할 것으로 사료된다.

가열시간에 따른 전단강도는 가열시간과 리플로 온도, 금속간 화합물의 두께에 의해 달라지며, 특히 금속간 화합물층의 증가는 솔더 범프의 강도 저하를 수반하는 것으로 사료된다.

본 연구 결과, 새로운 솔더링 공정 기법으로서 고주파 유도가열의 전자산업에 대한 적용 가능성과 신뢰성을 확인하였다.

Chapter 1. Introduction

1.1 Background

Soldering is the effective joining process in the assembly of semiconductor, and other parts of the electronic circuit system.

Recently, the trend in electronic device, such as laptop computer, mobile phone, is towards smaller and thinner size and integration. The soldering processes are being changed and developed according to these trends. In case of packaging methods that plays important role in soldering processes, the conventional DIP(Dual In-line Package) is changed into QFP(Quad Flat Package) and TSOP(Thin Small Outline Package) → BGA(Ball Grid Array) → CSP(Chip Scale Package). At the same time, assembling ways were also changed from through-put assembly technology(THT : Through Hole Technology) to surface assembly method(SMT : Surface Mounting Technology). Since a unit area of solder joints and joining object size decrease for the higher integration and density in advanced electronic products, the reliability of solder joints become a problem by meltage of solder joints, diffusion thickness and surface tension.

Accordingly, the conventional soldering methods such as Infrared Ray(IR), Hot Air, Vapor Phase Soldering(VPS) and laser Soldering are utilized but this study employed using the high-frequency induction heating as a new joining process. And the research for joining characteristics of solder bump according to the material property of pad carried out.

1.2 Purpose

Due to the environmental restriction against lead solder, it is required to develop

lead-free solder. In addition, new soldering technology, localization of material and development of new material have to be achieved, and the utilization and evaluation technology for those have to be established as well.

Since the conventional soldering bumping technology requires the expensive equipment, minimal pitch and limited yield of material, the approach to newly extensive bumping technology is required.

Europe has taken an aggressive position towards Pb-free legislation. The waste electrical and electronic equipment directive by EU has claimed that the use of Pb in consumer electronics will be banned after January 2006. There are impending producer responsibility laws for electronic and electrical equipment in a number of European countries. Such laws were passed in the Netherlands and Switzerland before 1999. Limits for recycling of specified materials may also be included.

The conventional equipment is focused on lead solder, therefore, a necessity of the new equipment for lead-free soldering is being raised in present.

However, the preparation for this new soldering process is insufficient in domestic.

In this study, induction heating reflow soldering was applied to soldering process for Pb-free solder and each substrate(such as Au/Ni/Cu, Au/Cu, Ni/Cu and Cu pad), experimented about the formation condition of solder bump, analysis of micro-structure, shear strength, IMC and influence of IMC.

The purpose of this study is prediction of the possibility and application for induction heating reflow soldering in the future electronic industries.

1.3 Research methods

The various processes are being used for the conventional soldering methods such as IR (Infrared Ray), Hot air, Laser, Hot plate and so on. The present soldering methods have many problems such as higher assembly density demand, multi-pin and smaller package. Especially, the assembly process of BGA (Ball Grid Array) has different characteristics of interface micro-structure and shear strength by each

solder ball's characteristics, property and reflow process. Therefore, in this study, induction heating reflow soldering is applied to a new soldering process. It is intended to develop a new joining process using high-frequency induction heating applied for melting of compound metal, forging, hardening and brazing.

1.3.1 Definition of induction heating

Induction heating is one of the high-frequency heating processes, is to heat material that is put inside of varying magnetic field and the material such as metal for induction heating has to be conductor. Heating material have not to have a property of magnetic substance, but has a conduction necessarily.

The heat emission distribution of induction heating heat from the surface of electrical load and induction heating is applied to melting of metal alloy, hardening, welding, brazing, casting, manufacture of single-crystallization and melting refine of Germanium and Silicon in semi-conductor field.

Alternating current(AC) used in induction heating and thickness of heating material have a close relation. A low-frequency is effective to thicker material but the high-frequency is effective to thinner and smaller material.

The heating time and the range of output power vary with the property of heating material and the induction coil shape. Since cooling water flows in the induction heating coil, it is made of copper pipe to prevent the corrosion and applicable to a various electronic parts.

1.3.2 Merit of induction heating

The merit of induction heating has a high efficiency because heated itself. In addition, the expense for soldering by induction heating will be reduced, because it heats specific area. Since it is possible to control the constant temperature and

melting point with an adequate frequency selected to the material and its size, A mass production and confirmative quality of solder bump will be achieved. Induction heating doesn't produce environment pollution and it is carried out in sanitary work because of detach between heating source and heating material. And the change in material is not developed by short working time and rapid work is possible because of no needs for preparation time such as preheating and slow cooling. Because the set-up area is small for output power, It has the spatial advantage.

In present, induction heating has been mainly applied to the brazing but it is considered that its application to the soldering is possible as a new technology.

1.3.3 Experiment

To establish the joining characteristics of lead-free solder ball by induction heating, first, the soldering of Sn-3.5Ag solder ball and FR4 substrates(such as Au/Ni/Cu, Au/Cu, Ni/Cu and Cu pad) was performed by induction heating. In order to determine the optimal initial condition for solder bump, the solder bump was formed such that the frequency is fixed and the current and time are varied. It was assumed that the influence of magnetic field is constant to the solder ball at entire area. The optimum soldering condition for each of pad was selected by induction heating reflow varying the current with time. On soldering by induction heating, the heating value of solder bump was measured by the infrared ray thermoscope.

Secondly, the measurement and analysis of Inter-Metallic Compound(IMC) were carried out by aging-test(0, 1, 4, 9, 16day) after soldering by induction heating and hot air reflow respectively. The metallic structure of interface was pictured by SEM and analyzed by EDS.

Third, the temperature gradient distribution of solder joints by induction heating were analyzed by the numerical simulation.

Forth, the soundness of solder bump for each pad was evaluated by measuring the shear strength in joining region and IMC thickness of the interface was measured.

Chapter 2. Solder bump formation by induction heating

2.1 Experiment

In this study, solder ball and substrate have been soldered by induction heating. The optimum soldering condition has been determined by the shape analysis and heating value of solder bump after soldering.

The solder ball and substrates used in this study are Sn-3.5Ag(melting point:221℃) of diameter 0.762㎜ and FR4 substrate(such as Au/Ni/Cu, Au/Cu, Ni/Cu and Cu pad). The water-soluble resin flux is spread on the substrate to protect oxidization and ethanol in ultrasonic waves equipment is used for removing the pollutants on the surface of specimen before spreading the flux for 10 minutes.

The optimum soldering condition for each of substrate and solder ball are selected by induction heating reflow varying the current with time. Table.2.1 shows the initial condition of induction heating reflow soldering.

Frequency (㎑)	Current (A)	Time (sec)
300	25, 27, 29	1, 1.5, 2, 2.5, 3, 4, 5

Table.2.1 The initial condition of induction heating reflow soldering

The FR4 substrate used in this study consisted of electroplates of 4 forms such as Cu(joined layer)/Ni(oxidization protection membrane)/Au(solder wetting layer), Au/Cu, Ni/Cu and Cu. Fig.2.1 shows the shape and dimension of FR4 substrates used for experiment.

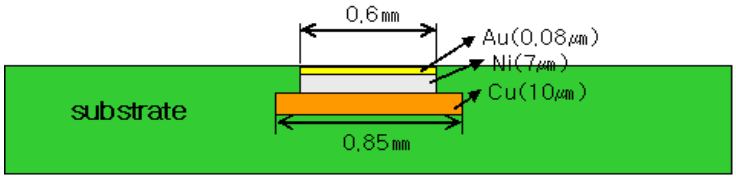

(A) Au/Ni/Cu

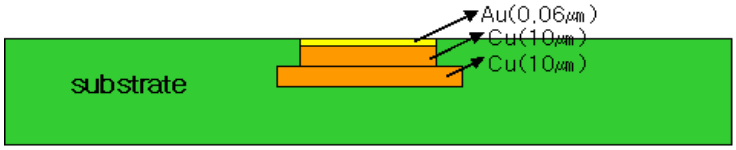

(B) Au/Cu

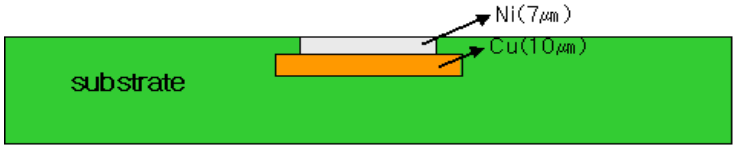

(C) Ni/Cu

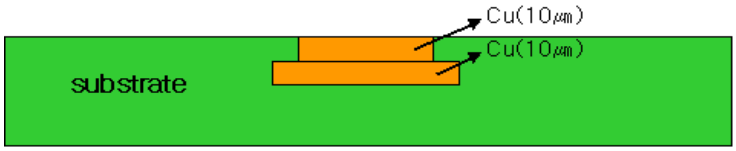

(D) Cu

Fig.2.1 The shape and dimension of FR4 substrate

Solder balls were dipped into water-soluble resin flux and were placed on the pads of substrates at the center of induction heating coil, manually. They are soldered on the upper plated layer of pads with time increment by self-alignment with the flux action between substrate and solder ball. The flux improves the wettability of solder by decreasing the surface tension between substrate and solder ball. The schematic diagram of induction heating system is shown in Fig.2.2.

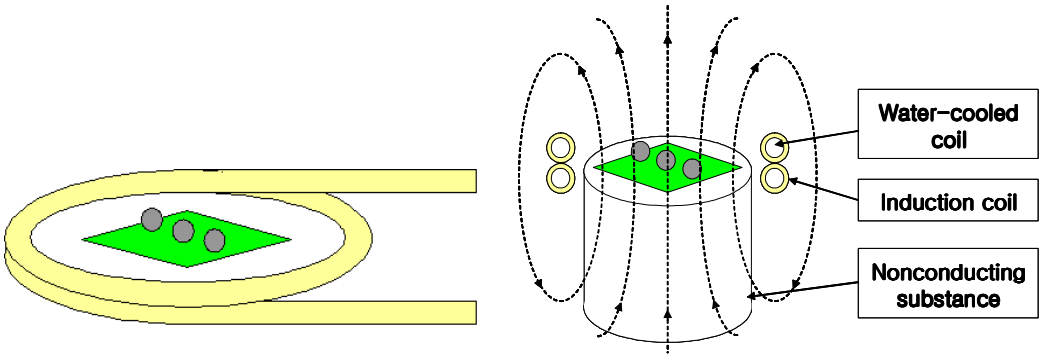

Fig.2.2 The schematic diagram of induction heating system

2.2 The heating value of solder bump by induction heating

To analyze the influence of each electroplate on the soldering by induction heating and search the optimum soldering condition for each of the substrate and the solder ball, induction heating reflow soldering was conducted by Table.2.1. Also, on reflow soldering, the heating value of solder bump was measured by the infrared ray thermoscope.

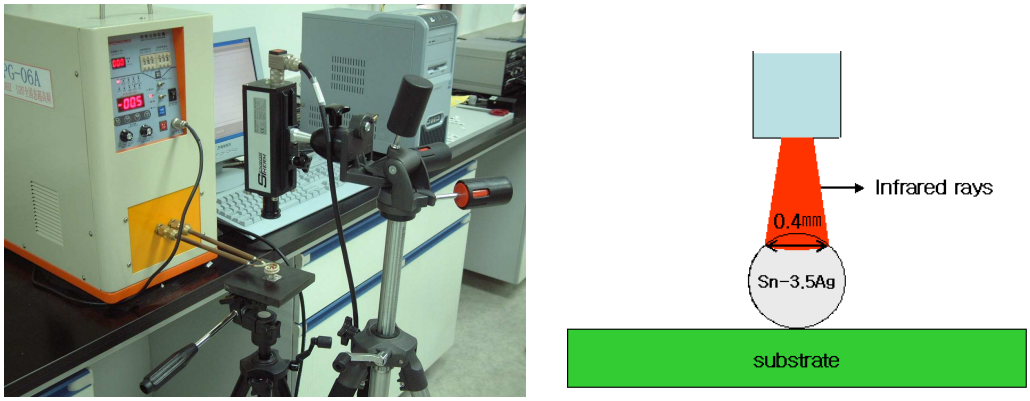

Fig.2.3 Thermoscope setup to measure heat value

Fig.2.3 shows the induction heating system, the infrared ray thermoscope and the schematic diagram of heating value measurement.

The heating values of the solder bumps between Sn-3.5Ag solder ball and each pad were obtained as shown in Table.2.2. while conducting the induction heating reflow soldering. The current was varied as 25A, 27A and 29A. The heating value measurement of the solder bump was carried out for heating time(1, 1.5, 2, 2.5, 3, 4, 5sec) with current and frequency being fixed. Fig.2.4 shows the solder bump temperature graph with respect to heating time for current(25, 27, 29A) based on Table.2.2.

	1 sec	*1.5 sec*	*2 sec*	*2.5 sec*	*3 sec*	*4 sec*	*5 sec*
25A	220.4℃ (non bumping)	238.4℃	265.7℃	305.8℃	338.1℃	379.9℃	420.1℃ (deformation)
27A	220.7℃ (non bumping)	242.5℃	275.8℃	333.5℃	367.7℃	420.9℃ (deformation)	461.8℃ (burned)
29A	226.8℃	257.2℃	305.2℃	354.1℃	384.2℃	447.6℃ (burned)	522.3℃ (burned)

(A) Au/Ni/Cu pad

	1 sec	*1.5 sec*	*2 sec*	*2.5 sec*	*3 sec*	*4 sec*	*5 sec*
25A	225.3℃	244.6℃	275.8℃	329.6℃	339.6℃	411.1℃	449.8℃ (burned)
27A	228.3℃	251.6℃	306.7℃	344.3℃	384.1℃	439.6℃ (burned)	479.4℃ (burned)
29A	229.5℃	261.6℃	311.5℃	359℃	405.2℃	452.3℃ (burned)	528.6℃ (burned)

(B) Au/Cu pad

	1 sec	*1.5 sec*	*2 sec*	*2.5 sec*	*3 sec*	*4 sec*	*5 sec*
25A	209.2℃ (non bumping)	235℃	250.9℃	288.3℃	317.8℃	361.5℃	414.4℃
27A	215.2℃ (non bumping)	240.2℃	269.3℃	293.2℃	337.8℃	395.2℃	420.5℃ (deformation)
29A	219.5℃ (non bumping)	248.8℃	285℃	336.9℃	364.4℃	389.9℃	462.1℃ (burned)

(C) Ni/Cu pad

	1 sec	*1.5 sec*	*2 sec*	*2.5 sec*	*3 sec*	*4 sec*	*5 sec*
25A	245.1℃	277℃	343.1℃	388.5℃	432.4℃ (deformation)	532℃ (burned)	
27A	250℃	289℃	373.4℃	424.5℃ (deformation)	475.1℃ (burned)		
29A	257.8℃	332.9℃	401.8℃	454.1℃ (burned)	556.9℃ (burned)		

(D) Cu pad

Table.2.2 The heating value of solder bump

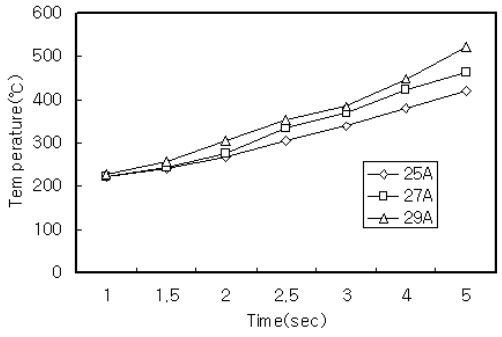

(A) Au/Ni/Cu

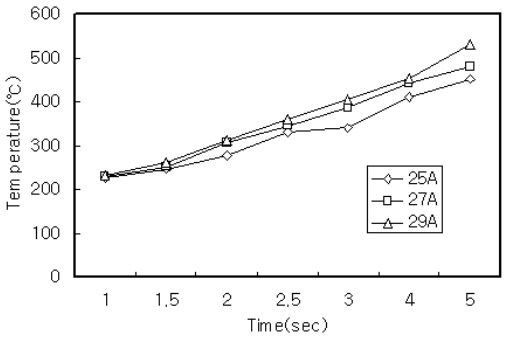

(B) Au/Cu

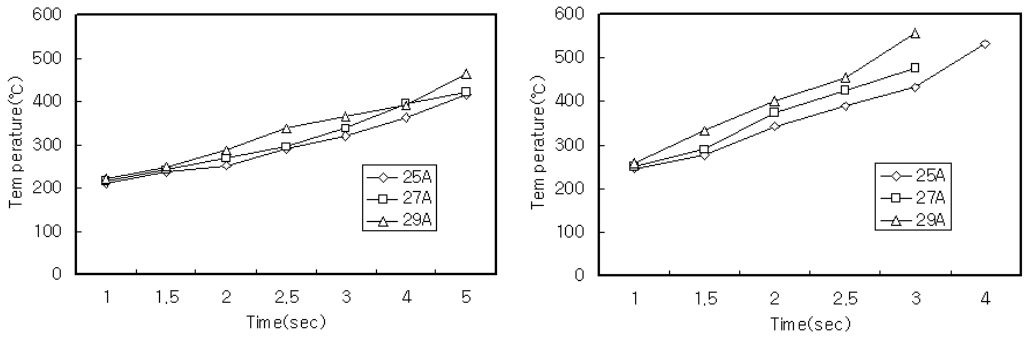

(C) Ni/Cu (D) Cu

Fig.2.4 The solder bump temperature graph with respect to heating time

The solder bump on Au/Ni/Cu pad could not be formed under 25~27A for 1sec and one on Ni/Cu pad could not be formed under 25~29A for 1sec, as the heating value was less than the melting point(221℃) of Sn-3.5Ag solder. Supplying more current, joining time was getting shorter, but if the heating time took a long time, we could see lots of substrate deformations and burns because of the heat concentration more than the thermal-resistance of substrate as shown in Fig.2.5. Cu pad showed the highest heating value and rapid substrate deformation due to the high increasing rate of temperature for time. Ni/Cu pad showed the lowest heating value. It has been found that the heating value of the solder bump was varied with respect to the thermal conductivity of the electroplate on the substrate. The conductivities of electroplates on substrates used in this study are shown in Table.2.3.

The range of minimizing the thermal influence for substrate is considered as 250~300℃. Therefore, the red boxes in Table.2.2, 1.5~2sec in case of Au/Ni/Cu pad and Au/Cu pad, 2~2.5sec in case of Ni/Cu pad and 1~1.5sec in case of Cu pad, are considered as the optimum condition of solder bump formation based on the heating value.

(A) Au/Ni/Cu (29A,5sec)

(B) Au/Cu (29A,5sec)

Fig.2.5 The deformation of substrate

Electroplate	Thermal conductivity (㎉/℃)
Cu	320
Au	254
Ni	77

Table.2.3 the thermal conductivity of the electroplates

Chapter 3. Micro-structure characteristics of solder bump

3.1 Interface reaction of solder bump

While solder is wetted on the surface of solid metal(lead, pad, etc), the atoms of liquid and solid metal are interact each other. Inter-Metallic Compound(IMC), the fusion of the atoms of solder and base metal, is produced by the diffusion. IMC is the stable compound composed of other atoms more than 2 sorts. Generally, since IMC is stiff and brittle, the strength, the conductivity and the corrosion resistance of solder joint are lowered. Also, since IMC has the high melting point and inferior metallic property and is subject to producing the stable oxide on surface, the wetting inferiority of solder occurs. The thickness of IMC is increased by higher temperature and longer heating time.

Due to the different thermal conductivity of IMC formed between solder and substrate and the incompatibility of metal structure, the stress concentrates between solder and substrate and decreases the reliability of the joint.

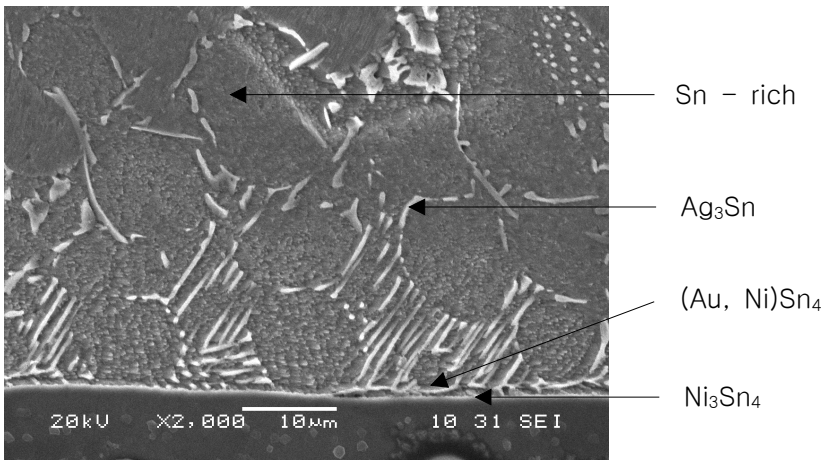

(A) Au/Ni/Cu pad (2sec)

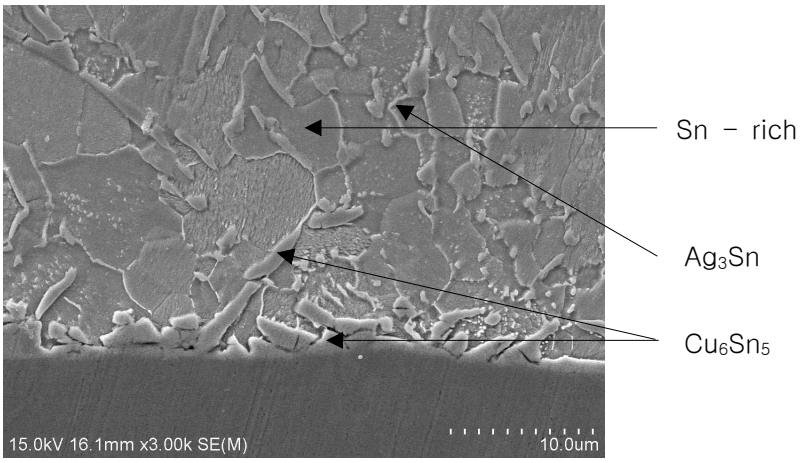

(B) Au/Cu pad (2sec)

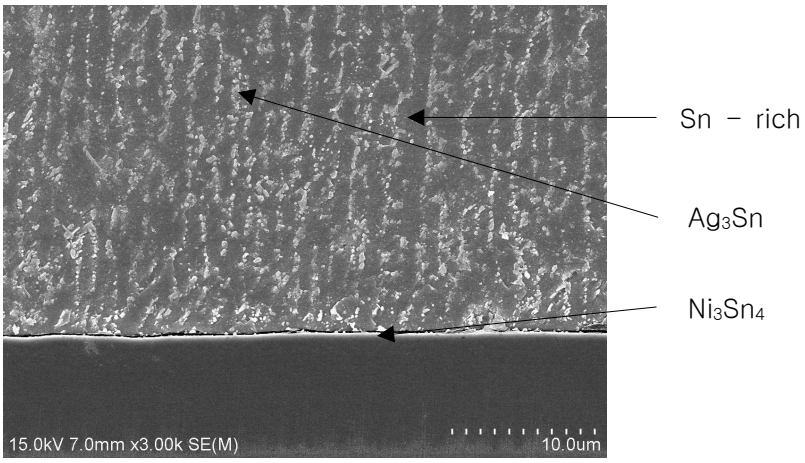

(C) Ni/Cu pad (2sec)

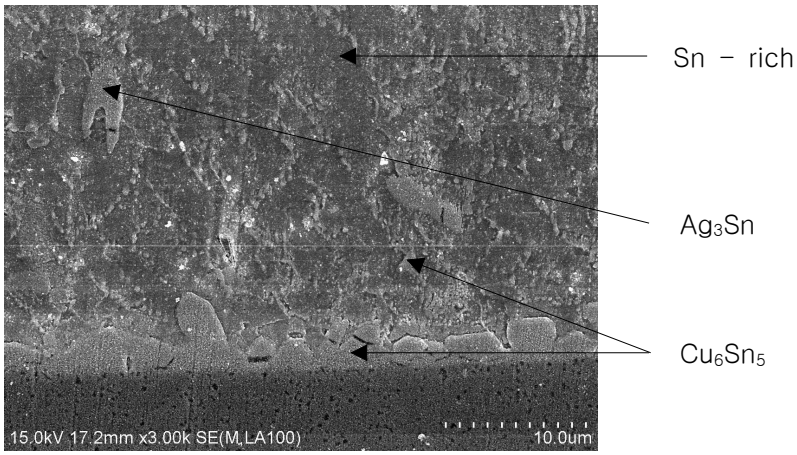

(D) Cu pad (2sec)

Fig.3.1 SEM image of the solder bump interface reflowed by induction heating

Fig.3.1 shows the interface structure of Sn-3.5Ag solder bump by induction heating varying the electroplate of pad. The reflow soldering condition is frequency : 300㎑, current : 29A and heating time : 2sec.

In the solder bump for each pad, the inside portion of solder ball is composed of pure Sn phase and Ag_3Sn. The compound created in the interface of solder bump varies based on the electroplate material of the pad.

In case of Au/Ni/Cu pad, Ni_3Sn_4 created by the interaction of Ni and Sn exists at the interface and a small quantity of Au is found just above this interface. In the solder bump for Au/Cu pad, Cu_6Sn_5 is created mainly at the interface. Ni_3Sn_4 is created in the interface between Sn-3.5Ag solder and Ni/Cu pad as Au/Ni/Cu pad and Cu_6 Sn_5 exists at the inside of solder and the interface of Cu pad. Cu_6Sn_5 in the solder is created by Cu melted from Cu layer of substrate or separation from IMC at the interface. Since Sn-Cu inter-metallic compound is more brittle than Sn-Ag inter-metallic compound, The decrease of IMC in interface increases the strength and fatigue life of solder joint.

3.2 Metallurgical change with aging day

In this study, the measurement and analysis of Inter-Metallic Compound between Sn-3.5Ag solder and Au/Ni/Cu pad were carried out by aging-test considering the initial condition established at the proceeding chapter. And the micro structure of solder bump by induction heating was compared with the structure of solder bump by Hot-air reflow. The process of experiment and material are identical with the previous test. With the selected condition of induction heating, the metallic structure analysis was carried out with aging day as shown in Table.3.1

After soldering, the specimens were aged at temperature 120℃ using the furnace and then mounted and polished. After etching the specimens for 5 seconds with solvent 74% CH_3CH_2OH, 1% HCl, 5% HNO_3 and 20% H_2O, the metallic structure of interface is captured by SEM(Scanning Electron Micrography) and analyzed by EDX(Energy Dispersive X-Ray).

Solder ball	Induction heating	Hot-air reflow	Aging
Sn-3.5Ag	300㎑ 29A 2sec	250℃	120℃ 0, 1, 4, 9, 16days

Table.3.1 The aging condition for experiment

3.2.1 The micro structure and interface of Sn-3.5Ag solder bump related to aging

Sn-3.5Ag(melting point : 221℃) solder has more excellent tensile strength and thermal fatigue creep characteristics than that of Sn-37Pb solder. Due to the low

migration sensitivity, the jointed area has the excellent reliability and as the service life increases, the strength value decreases.

As shown in Fig.3.2, Ag_3Sn (rod-like type) exists in the solder ball at the initial stage and (Au, Ni)Sn_4 and Ni_3 Sn_4 appear after aging time. (Au, Ni)Sn_4 and Ag_3Sn compound coexist in some solder part. As aging time increases, Au plated on the substrate shows a tendency to move into solder ball and IMC of Ni exists around the interface, as Ni functions as a protection layer between solder and Cu layer.

Ag_3Sn created at the Sn base grows to the direction of solidification. Also, on soldering, the nucleus creation of Ag_3Sn is accelerated by high heating and rapid cooling rate but the structure has minute variation as the growth of Ag_3Sn is prevented. Where as in the opposition case Ag_3Sn grows into rod-like type. Ag_3Sn develops in the solder ball at the initial stage and spreads to the small area because it stabilizes with aging time. Ag_3Sn is not coarsened at high temperature and has the excellent reliability. Sn-rich phase occupies most of the solder ball and the uneven phase at the initial interface stabilizes to the even phase with aging time.

Fig.3.3 shows the interface captured by SEM for different aging times.

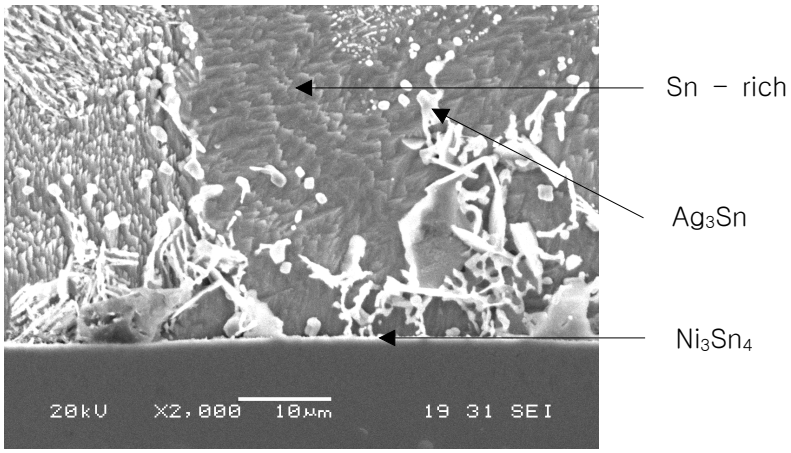

(A) Induction heating (Au/Ni/Cu pad, 0 day)

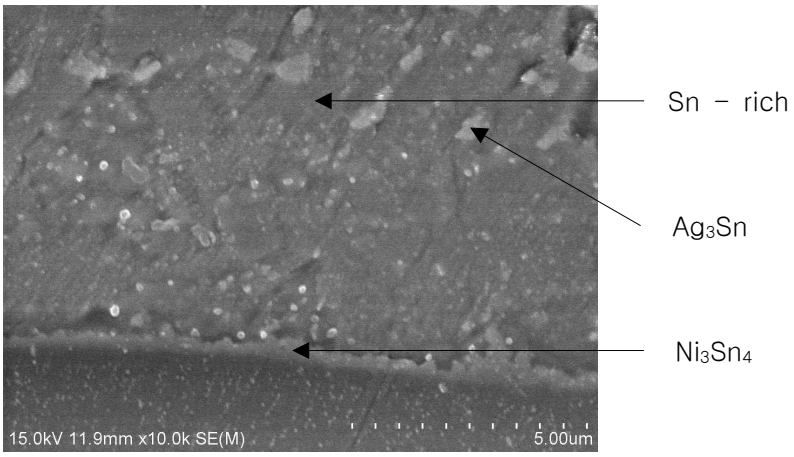

(B) Hot air reflow (Au/Ni/Cu pad, 0 day)

Fig.3.2 SEM image of the solder bump interface by two soldering processes

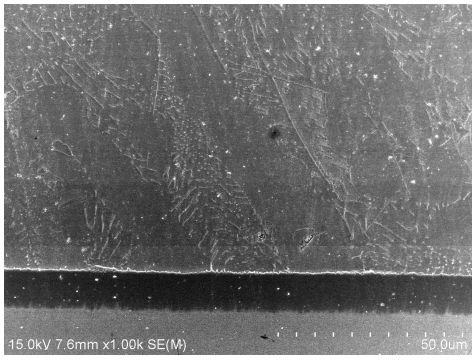

(A) Induction heating (1 day)

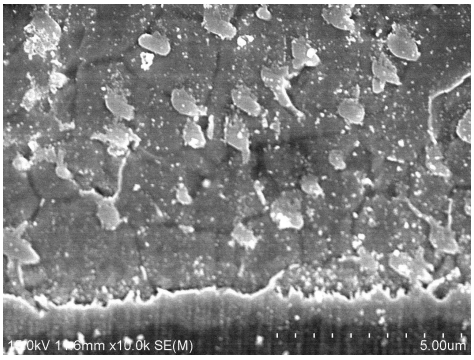

(B) Hot air reflow (1 day)

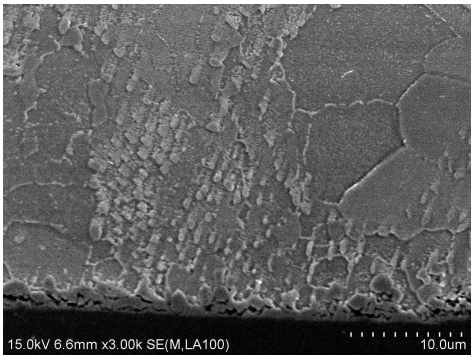

(C) Induction heating (4 day)

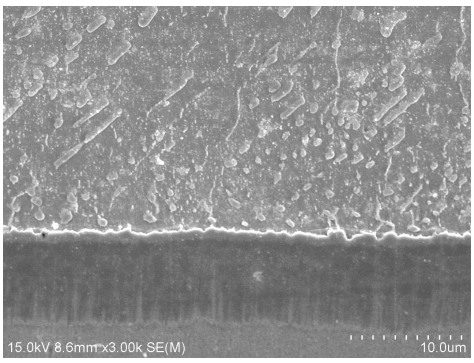

(D) Hot air reflow (4 day)

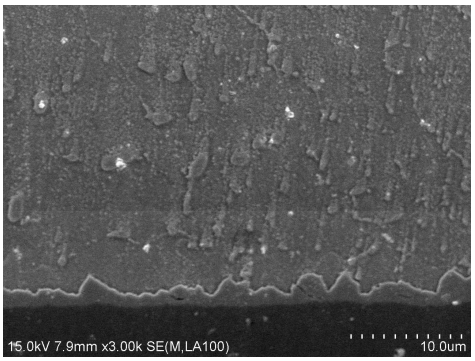

(E) Induction heating (9 day)

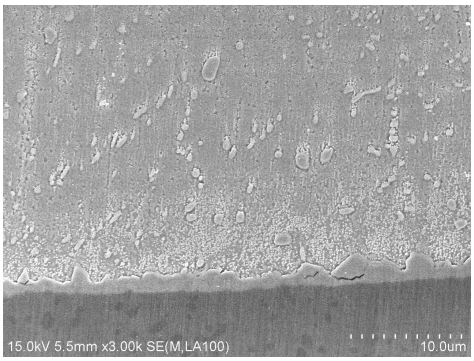

(F) Hot air reflow (9 day)

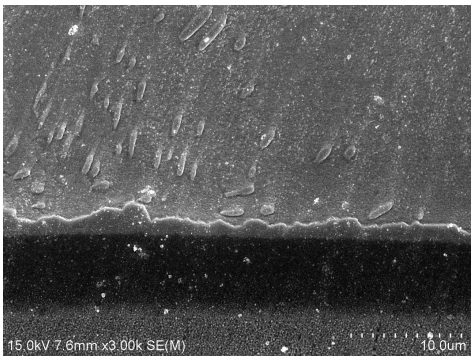

(G) Induction heating (16 day)

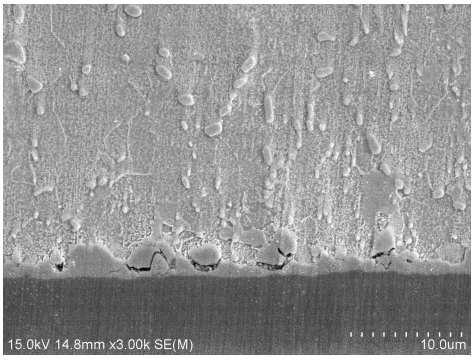

(H) Hot air reflow (16 day)

Fig.3.3 SEM image of the solder bump interface for various aging days (Au/Ni/Cu pad)

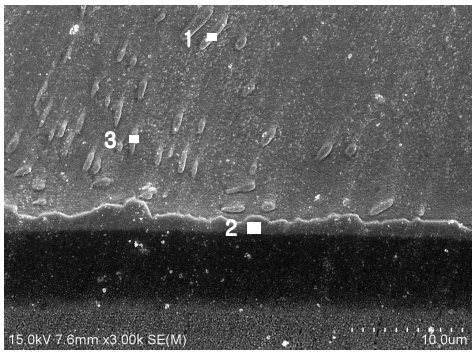

Point	1		2		3	
Element	Wt%	At%	Wt%	At%	Wt%	At%
SnL	74.68	72.84	95.64	91.55	85.03	74.47
AgL	25.32	27.16				
AuM					0.79	0.41
NiK			4.36	8.45	14.19	25.12

(A) Induction heating (16 day)

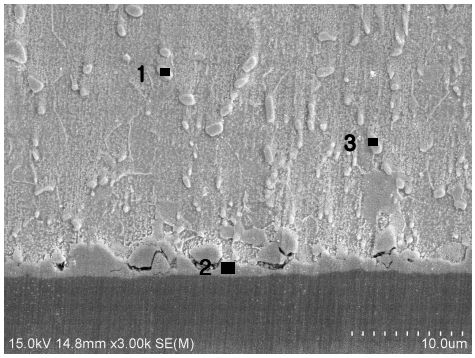

Point	1		2		3	
Element	Wt%	At%	Wt%	At%	Wt%	At%
SnL	28.03	26.14	61.64	44.68	82.60	80.76
AgL	71.97	73.86			15.60	16.79
AuM			0.86	0.38	0.78	0.46
NiK			37.50	54.94	1.01	2.00

(B) Hot air reflow (16 day)

Fig.3.4 The EDX analysis of Sn-3.5Ag solder bump

Fig.3.4 shows the constituent analyzed by EDX in solder structure after 16 days. (Au, Ni)Sn_4 composed of (Au, Ni)Sn_4 and Ag exists on Ni_3Sn_4 at the interface. Ag_3Sn exists in the solder ball.

Fig.3.5 shows the Phase diagram of Au-Sn, Ni-Sn and Ag-Sn binary alloy.

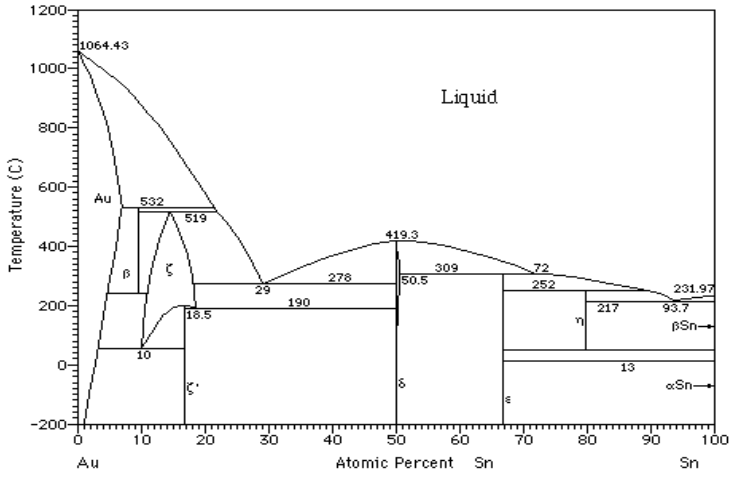

(A) Phase diagram of Au-Sn binary alloy

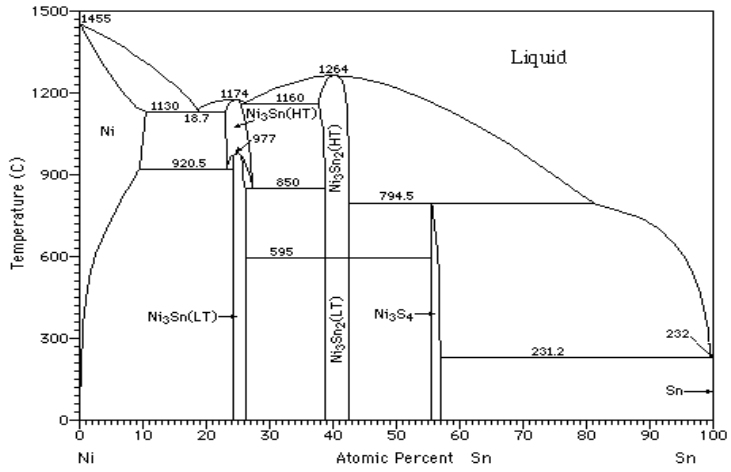

(B) Phase diagram of Ni-Sn binary alloy

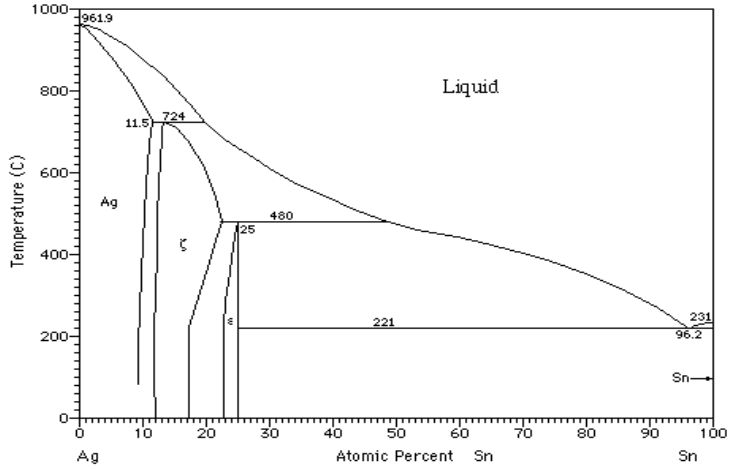

(C) Phase diagram of Ag-Sn binary alloy

Fig.3.5 Phase diagram of binary alloy (Au-Sn, Ni-Sn, Ag-Sn)

Chapter 4. Thermal analysis of solder bump

In this study, the simulation for temperature gradient distribution of Sn-3.5Ag solder bump by induction heating is conducted using Nastran, the numerical analysis program. The problem of heat conduction is formulated using finite element method based on Galerkin method in two dimensional steady state heat conduction equation and the interrelation between the result of simulation, creation of IMC and structure around interface are investigated by simulation.

4.1 Basic theory

Boundary condition is given in Fourier's law, the following form using the heat flux q (cal/cm3 · sec · ℃) in normal direction on the boundary of the object.

$$q = -\lambda_x \frac{dT}{dx} \qquad (4 \cdot 1)$$

where q : heat flux

$\frac{dT}{dx}$: temperature gradient

T : temperature

x : the direction of heat flow in orthogonal

λ_x : thermal conductivity (㎉/m · hr℃)

Then by equation (4 · 1), the rate of heat conduction in the three directions (x, y, z) per unit volume becomes

$$\frac{\partial}{\partial x}(\lambda x \frac{\partial T}{\partial x}) + \frac{\partial}{\partial y}(\lambda y \frac{\partial T}{\partial y}) + \frac{\partial}{\partial z}(\lambda z \frac{\partial T}{\partial z}) \qquad (4 \cdot 2)$$

Due to the assumption for constancy of temperature by time, the rate of time change of internal energy per unit volume is not considered.

$$0 = \rho c \frac{\partial T}{\partial t} \qquad (4 \cdot 3)$$

From conservation of energy, the fundamental equation of heat conduction is obtained as equation (4 · 4)

$$0 = \frac{\partial}{\partial x}(\lambda x \frac{\partial T}{\partial x}) + \frac{\partial}{\partial y}(\lambda y \frac{\partial T}{\partial y}) + \frac{\partial}{\partial z}(\lambda z \frac{\partial T}{\partial z}) + Q \qquad (4 \cdot 4)$$

where T : temperature (℃)

Q : rate of temperature change due to heat generated per volume (cal/sec)

If the solid is isotropic media ($\lambda_x = \lambda_y = \lambda_z = \lambda$), equation (4 · 4) can be written

$$0 = \lambda(\frac{\partial^2 T}{\partial x^2}) + \lambda(\frac{\partial^2 T}{\partial y^2}) + \lambda(\frac{\partial^2 T}{\partial z^2}) + Q \qquad (4 \cdot 5)$$

In this study, the two dimensional heat conduction analysis is considered, therefore, the equation (4 · 5) becomes two dimensional steady state heat conduction equation (4 · 6)

$$0 = \lambda(\frac{\partial^2 T}{\partial x^2}) + \lambda(\frac{\partial^2 T}{\partial y^2}) + Q \qquad (4 \cdot 6)$$

If Galerkin method is applied into (4 · 6), the equation can be written

$$\int_v [N]^T \left\{ \lambda \left(\frac{\partial^2 T}{\partial x^2} + \frac{\partial^2 T}{\partial y^2} \right) + Q \right\} d\,V = 0 \qquad (4 \cdot 7)$$

where, after conducting the partial differentiation to above equation (4 · 7) using Green-Gauss theorem, if equation (4 · 1) is substituted, steady state heat conduction equation can be expressed simply as finite element formular (4 · 8).

$$[k]\,\{\phi\} = \{f\} \qquad (4 \cdot 8)$$

where

$[k]$: heat conduction matrix

$$-\int_v \lambda \left(\frac{\partial [N]^T}{\partial x} \frac{\partial [N]}{\partial x} + \frac{\partial [N]^T}{\partial y} \frac{\partial [N]}{\partial y} \right) d\,V$$

$\{f\}$: heat flux vector

$$\int_s \alpha_c\, T_c\, [N]^T d\,S + \int_v \dot{Q}\, [N]^T d\,V$$

$\{\phi\}$: nodal temperature

In this study, the heat transfer analysis is carried out using the two dimentional heat conduction program by equation.

4.2 Finite element model and condition for simulation

The model used in this analysis is shown in Fig.4.1 and the total number of element and node are 207,798 and 209,242 respectively.

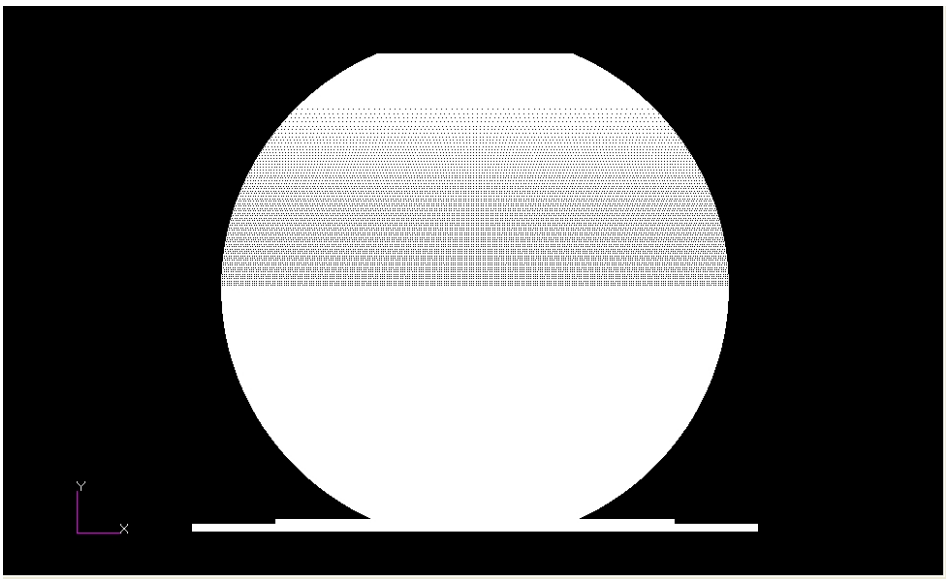

Fig.4.1 The schematic mesh division for F.E analysis

In this study, following conditions are considered for accurate heat conduction analysis.

1) Two dimensional steady state heat conduction analysis has been conducted using 4-node iso-parametric element.
2) The thermal coefficient of material varies with the temperature and the thermal conduction is treated as non-linear function.
3) The material is iso-tropic media and the initial temperature is 20℃.

Induction heating reflow condition used in this simulation are frequency : 300㎑, current : 29A, heating time : 2sec for each pad. The actual heating value of solder bump by identical soldering condition in chapter 2 is considered as heat input for simulation. Table.4.1 shows the actual heating value of solder bump considered as heat input for each pad and the physical property of material varied with the temperature is shown in Table.4.2

Pad type	Heating value (Heat input)	Soldering condition
Au/Ni/Cu	305.2℃	frequency : 300㎑ current : 29A heating time : 2sec
Au/Cu	311.5℃	
Ni/Cu	285℃	
Cu	401.8℃	

Table.4.1 The heat input for the simulation
(The actual heating value by the infrared ray thermoscope)

Material	Thermal conductivity (micro-W/mm · ℃)	Temp
Sn-3.5Ag solder	5.7309×10^4	Room teperature
Gold (Au)	3.1790×10^5	
Nickel (Ni)	9.1858×10^4	
Copper (Cu)	3.8696×10^5	

Table.4.2 The physical property of the Sn-3.5Ag solder and the electroplates

4.3 Temperature gradient distribution of solder bump

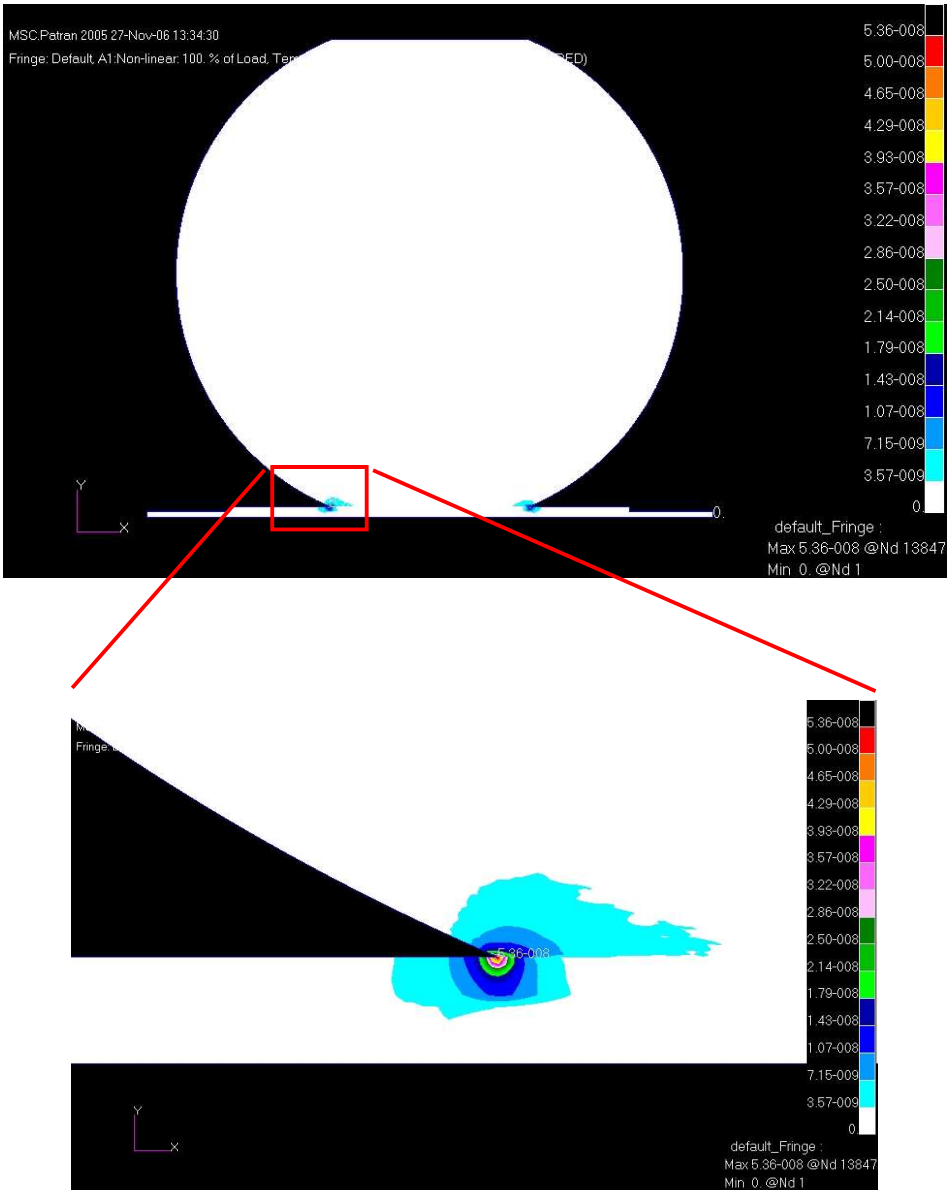

Fig.4.2 Temperature gradient of Sn-3.5Ag solder bump for Au/Ni/Cu pad

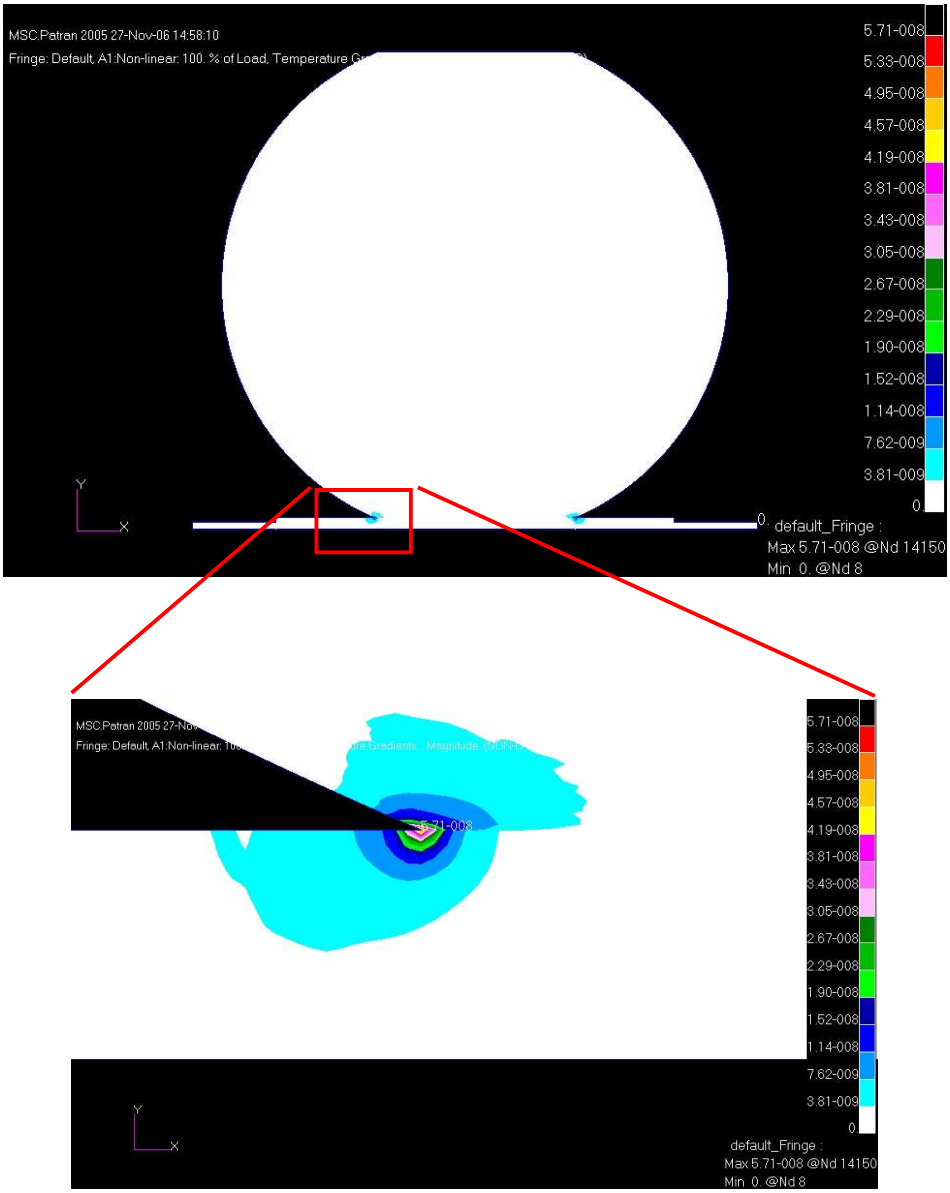

Fig.4.3 Temperature gradient of Sn-3.5Ag solder bump for Au/Cu pad

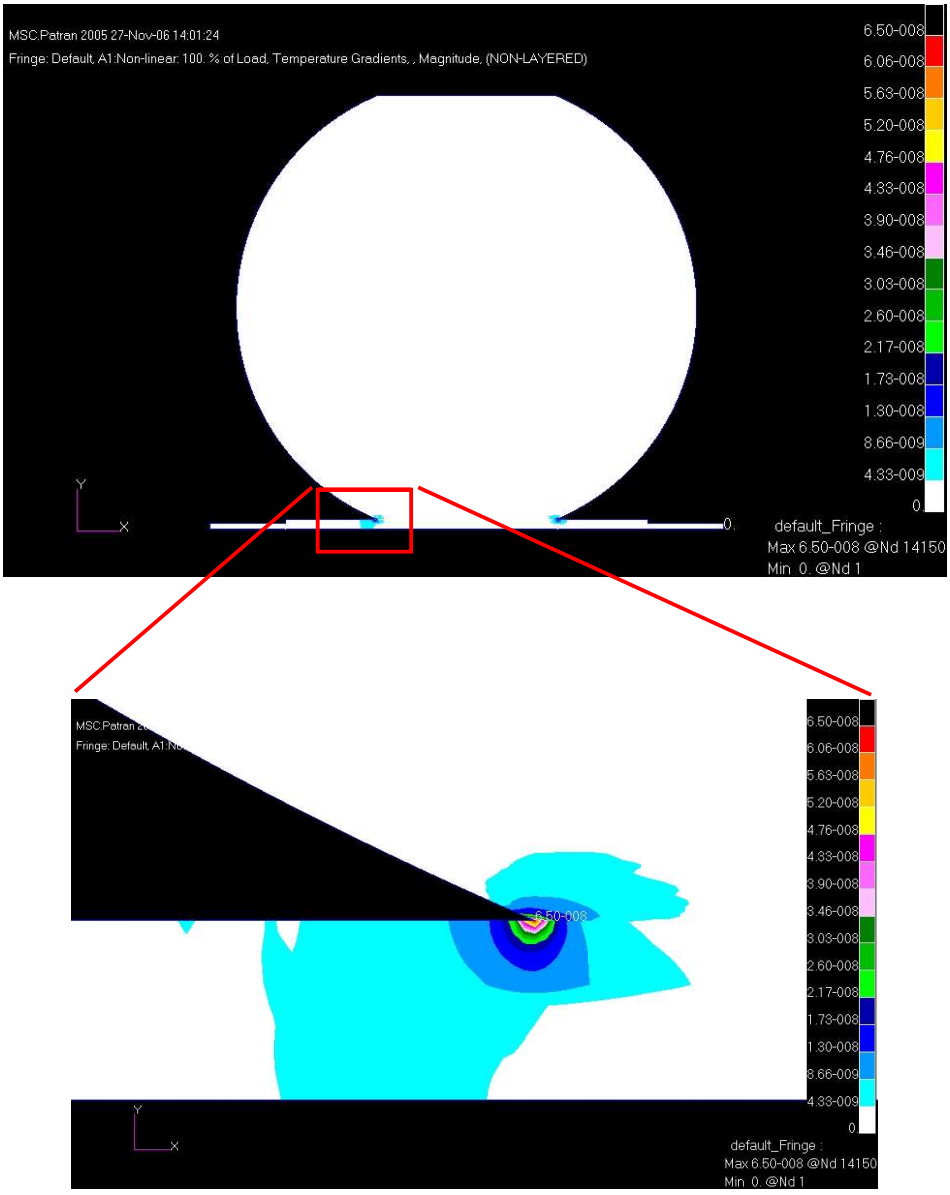

Fig.4.4 Temperature gradient of Sn-3.5Ag solder bump for Ni/Cu pad

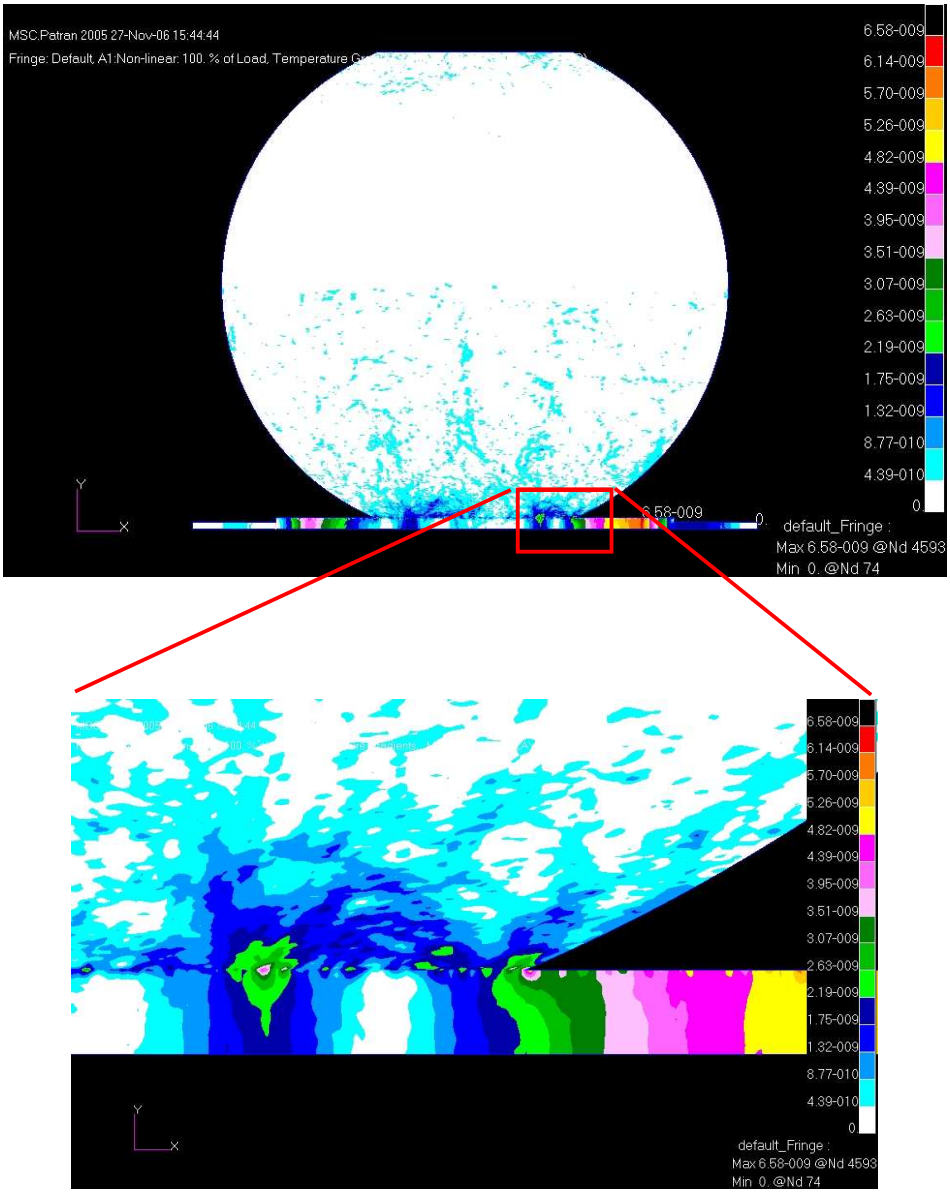

Fig.4.5 Temperature gradient of Sn-3.5Ag solder bump for Cu pad

The temperature gradient distribution of solder bump for each pad simulated using Nastran, the numerical analysis program, is shown in Fig.4.2, Fig.4.3, Fig.4.4 and Fig.4.5. Except for Cu pad, the simulations for each solder bump show the highest temperature gradient at both edges of joining interface and temperature is the highest at those areas. This phenomenon is caused by the geometrical and material non-linearity of these areas, therefore, the residual stresses are high at both edges of interface of solder bump.

In the solder bump for Cu pad, the temperature gradient distribution is broader than others and high temperature gradients are observed inside the solder in addition to interface. Especially, the highest temperature gradients are observed around pad and interface.

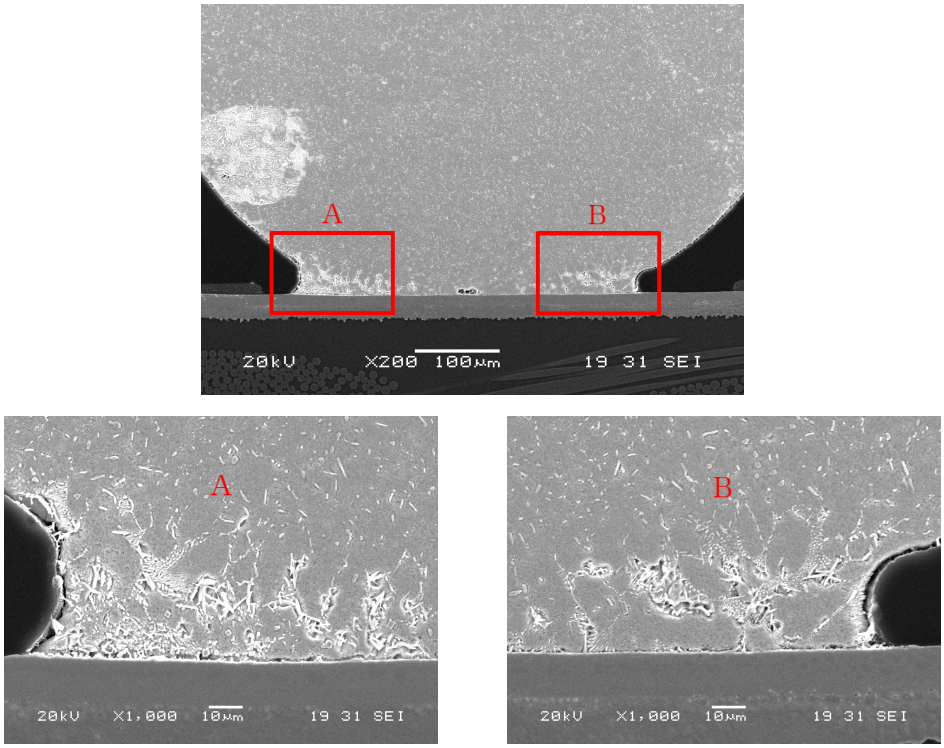

Fig.4.6 SEM image of the solder bump for Au/Ni/Cu pad by induction heating (300㎑, 29A, 2sec)

Fig.4.6 shows SEM image of the solder bump for Au/Ni/Cu pad by induction heating under the identical soldering condition(300㎑, 29A, 2sec) with the simulation. The interface state of solder bump in Fig.4.6 corresponds with the result of simulation in Fig.4.2. Fig.4.6 shows IMC grew bigger at both edges of interface than the inside of solder. The temperature is high at both edges of interface with the highest temperature gradient, therefore, the diffusion in this area between solder and electroplate is more active than other areas.

Chapter 5. The joint reliability

5.1 The shear strength of solder bump

5.1.1 The shear strength characteristics of solder bump

The shear strength of BGA(Ball Grid Array) joints in packaging assembly generally depends on various condition such as joining methods, joining temperature, heating time, conveyer speed, difference of specimen surface state and defects of joining interface.

Even though experimented values are varied by changing the joining conditions, in this present study, this variation was not accounted and the soundness of reflow soldering was evaluated by measuring the shear strength in joining region.

The solder ball used for this experiment are Sn-3.5Ag of diameter 0.762㎜ and the substrate is FR4 composed of Au/Ni/Cu, Au/Cu and Ni/Cu pad. To eliminate the foreign particles on the substrate, The substrate was cleaned for 10min using ethanol in the ultra wave equipment and then dried in the air.

As detailed in the Table.5.1, The solder ball was dipped into the water-soluble resin flux on the substrate manually and induction heating reflow soldering was carried out for Sn-3.5Ag solder ball and each type of pads with same test condition.

Electroplate	Induction heating	Heating time	Shear test
Au/Ni/Cu	frequency : 300㎑ current : 29A	1, 1.5, 2, 2.5, 3sec	tip height : 100㎛ tip speed : 1㎜/min
Au/Cu			
Ni/Cu			

Table.5.1 The shear test condition

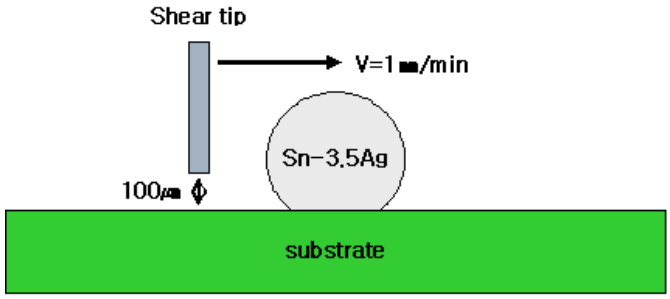

Fig.5.1 The schematic diagram of solder ball shear test

Fig.5.1 shows the schematic diagram of solder ball shear test. The tests were carried out about solder bump using the shear tip movement in the direction of an arrow as shown in Fig.5.1. The load speed of shear tip is 1㎜/min and the distance between tip and substrate is 100㎛.

Generally, the shear strength is related to thickness of IMC layer. The shear strength increases with increase in IMC layer thickness up to a critical value and further increase in IMC layer thickness above the critical value decreases the shear strength. In this study, a new soldering process is introduced and the shear strength variation has been plotted graphically.

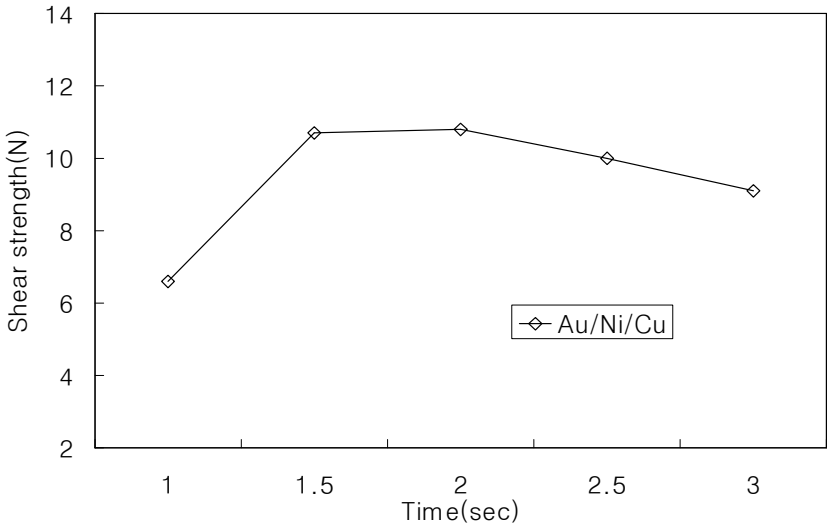

(A) Au/Ni/Cu pad

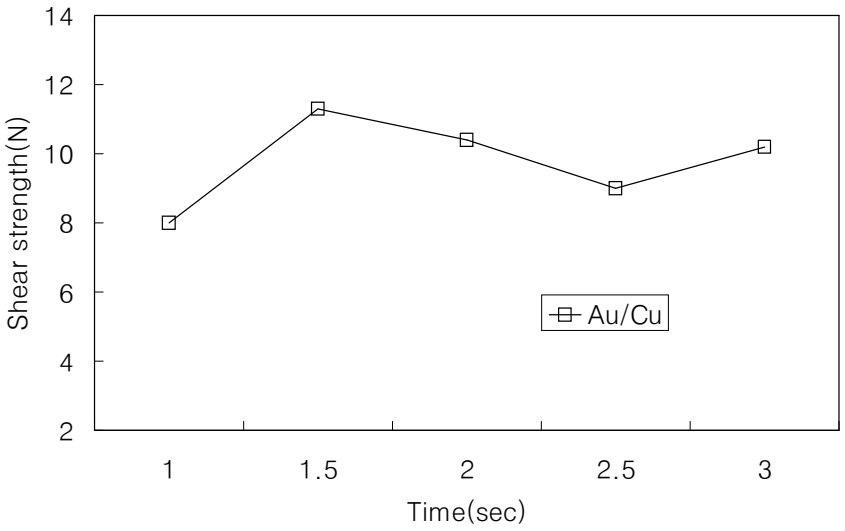

(B) Au/Cu pad

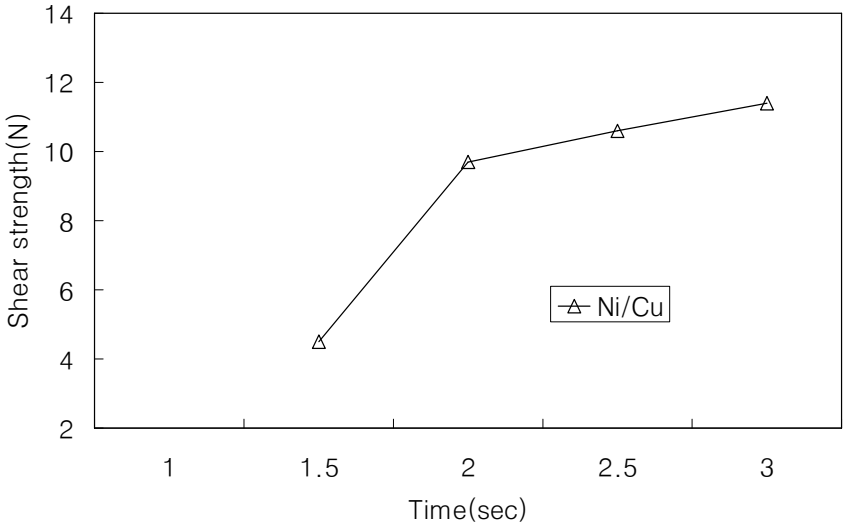

(C) Ni/Cu pad

Fig.5.2 The shear strength of Sn-3.5Ag solder bump for pad and heating time

As shown in Fig.5.2, the shear strength of Sn-3.5Ag solder bump by induction heating, varying pad and heating time, is increased at the initial stage but decreased as the heating time increases. The shear strength values are increased with the increment of IMC thickness up to some limit but decreased over limit.

The shear strength of solder bump for Au/Ni/Cu pad is about 6.6N at heating for 1sec and shows higher value at 1.5～2sec. The highest value is 10.8N at 2sec and the shear strength decreases on further increment of heating time.

The average shear strength value of the solder bump for Au/Cu pad is higher than Au/Ni/Cu, but lower than Au/Ni/Cu after 2sec. This is due to the influence of Ni and Cu that compose the pad. Au layer, wetting area of both pads, moves from the interface to the inside of solder as the heating time increases and Ni and Cu create IMC at the interface. Because the diffusion rate of solder in Ni is lower than Cu, Ni layer functions as the layer for diffusion prevention to restrain the creation of Cu-Sn compound. Therefore, the shear strength of solder bump for Au/Cu pad is higher than Au/Ni/Cu at the initial stage but becomes low by the increment of IMC thickness as the heating time increases. In case of Au/Cu pad, the highest strength is 11.3N at heating time of 1.5sec. The shear strength is observed to decrease as the heating time increases, same as Au/Ni/Cu pad, but shows irregular tendency.

The shear strength of solder bump for Ni/Cu pad increases continuously with the increment of heating time. The solder bump for Ni/Cu pad is not formed at 1sec due to low heating value and wettability of Ni layer. The shear strength is very low at the initial stage and is increased by the influence of Ni-Sn compound with the increment of heating time. The highest strength is 11.4N at 3sec and is higher than other pads.

IMC is very important for the reliability of solder bump because IMC causes the crack and fracture between solder ball and substrate, and besides, it inversely has an influence on the shear strength of solder joint.

5.2 Inter-Metallic Compound(IMC) thickness

IMC is created at joint between solder ball and substrate during soldering or using electronic equipments after soldering. Sn-group solder generates IMC by reaction with substrate and lead during soldering. IMC thickness increases with the increment of soldering and aging temperature. The joining strength is deteriorated by the brittleness of IMC with increment of IMC thickness. IMC affects the mechanical properties of solder joints, that is, it lowers the wetting, increase its electric resistance and brittle fracture, as a result, the reliability of solder joints is deteriorated.

IMC thickness at the interface is measured considering the average value between solder and interface. The variation of IMC thickness by heating time are given in Table5.2. Fig.5.3 shows the tendency of Table.5.2 graphically.

Pad	1 sec	1.5 sec	2 sec	2.5 sec	3 sec
Au/Ni/Cu	0.734㎛	1.130㎛	1.289㎛	1.482㎛	1.428㎛
Au/Cu	1.887㎛	1.948㎛	2.058㎛	2.075㎛	2.385㎛
Ni/Cu		1.013㎛	1.447㎛	1.845㎛	2.086㎛

Table.5.2 The IMC thickness by heating time

IMC thickness of each solder bump increases with the increment of heating time. In case of Au/Ni/Cu pad, IMC thickness is smaller than others for the heating time of 1sec. IMC for Au/Cu pad is thicker than others because the diffusion rate of solder is better in Cu than Ni. In case of Ni/Cu pad, the increasing rate of IMC thickness is the biggest. Comparing with Fig.5.2, the shear strength decreases with the increment of IMC thickness. The increment of IMC thickness by heating time has an effect on the shear strength of the solder joint.

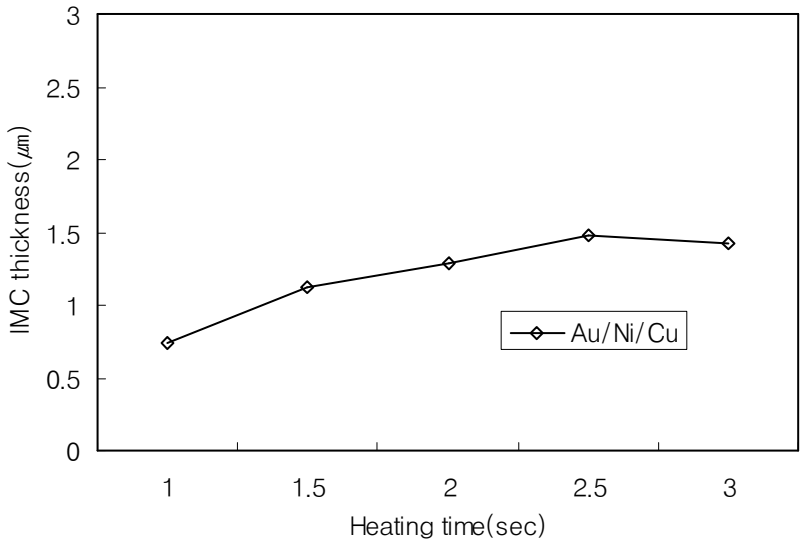

(A) The IMC thickness of solder bump for Au/Ni/Cu pad

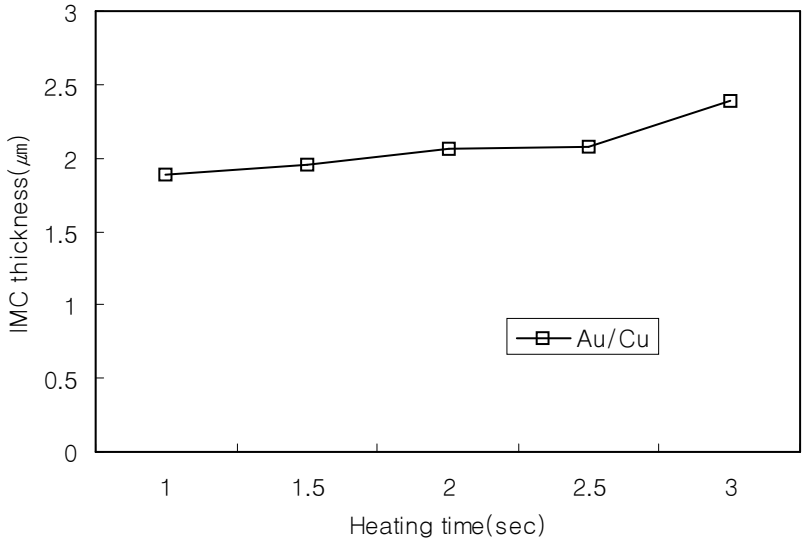

(B) The IMC thickness of solder bump for Au/Cu pad

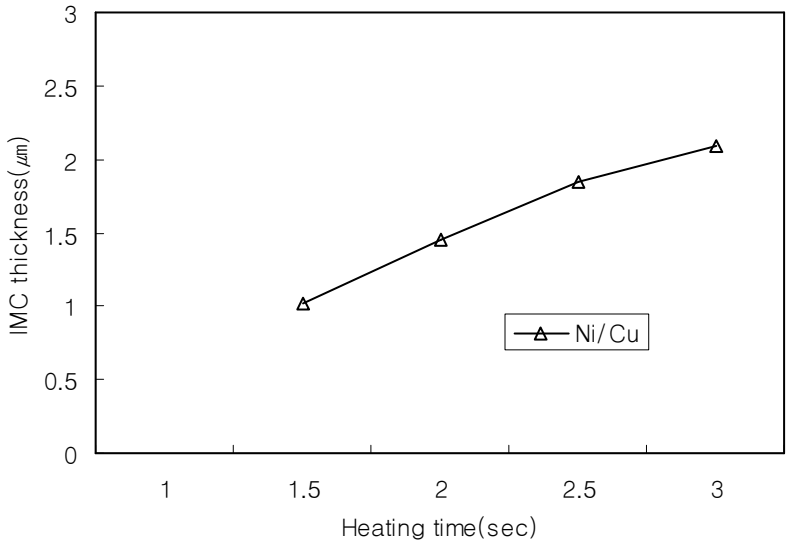

(C) The IMC thickness of solder bump for Ni/Cu pad

Fig.5.3 The IMC thickness on the interface by heating time

The variation of IMC thickness by aging time under the condition of Table.3.1 in Chapter 3 is given in Table5.3. The aging temperature is 120℃. The comparison of IMC thickness of solder bump by two reflow soldering processes, Induction heating reflow and Hot air reflow, is conducted considering aging time. Fig.5.4 expresses the graphical representation of Table.5.2.

Reflow process	0 (days)	1 (days)	4 (days)	9 (days)	16 (days)
Induction heating	1.155㎛	2.124㎛	2.462㎛	3.120㎛	3.910㎛
Hot air reflow	1.143㎛	2.139㎛	2.694㎛	3.202㎛	3.537㎛

Table.5.3 The IMC thickness by aging days (Aging temperature : 120℃)

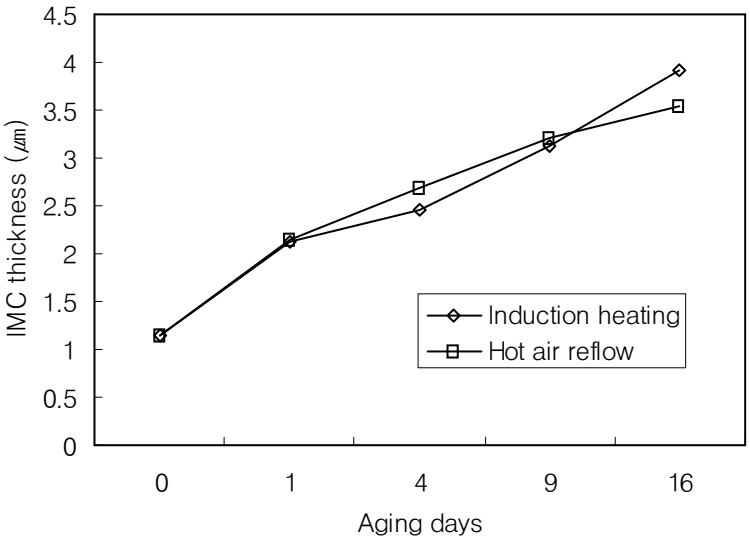

Fig.5.4 The IMC thickness on the interface by aging days

IMC thickness of solder bump by two soldering process shows the tendency to increase with increment of aging time. IMC thickness by two soldering processes is similar at the initial stage but IMC thickness by Hot air reflow is thicker with the increment of aging time than induction heating. After 16 aging days, IMC thickness by induction heating is thicker than Hot air reflow and the thickness is about 3.910㎛.

IMC thickness is closely related to the strength of solder joint and increases with the increment of heating time or aging time. The increment of IMC thickness causes the deterioration of solder joint.

Chapter 6. Conclusion

The results of this study about the joining characteristics of solder bump between Sn-3.5Ag solder ball and the various electroplates using the high-frequency induction heating as a new soldering process for Pb-free soldering are as follows. The new soldering process by induction heating confirmed the application possibility in electronic industries in the near future.

1. Formation of solder bump

1) The current, heating time and frequency are the main process variables for the formation of solder bump by induction heating.
2) From the measured results, due to the difference in the thermal conductivity of electroplates, the heating value of solder bump for Cu pad is the highest and Ni/Cu pad is the lowest. The thermal conductivity of electroplates have an effect on joining time.
3) Considering the heating value of solder bump and the range of minimizing heat affect on substrate, the optimum condition of solder bump formation for each of the pad are frequency : 300㎑, current : over 25A, heating time : 1.5sec~2.5sec.

2. Structure characteristics of solder bump

1) Each solder bump has different characteristics of interface structure based on the electroplates of each pad. Ag_3Sn on Sn base is observed as rod-like type at the inside of solder. Ni_3Sn_4 is observed at the interface of solder bumps for Au/Ni/Cu pad and Ni/Cu pad. Cu_6Sn_5 exists at the interface of solder bumps for Au/Cu pad and Cu pad. Au is observed around the interface due to the diffusion of Au into solder.

2) The uneven phase at the initial interface stabilizes to the even phase with aging time. Ag_3Sn in the solder ball has minute spreading as it stabilizes with aging time.

3. Temperature gradient distribution of solder bump

1) From the results of 2-D steady state heat conduction analysis, the high temperature gradient is observed around the interface of solder bump. Especially, Au/Ni/Cu, Au/Cu and Ni/Cu pads show the highest temperature gradient at both edges of joining interface due to the geometrical and material non-linearity at those areas, therefore, the residual stress is concentrated at both edges of interface between solder ball and pad.

4. Shear strength of solder bump, IMC thickness

1) The shear strength of Sn-3.5Ag solder bump by induction heating varies with pad properties and heating time and increases at the initial stage, but decreases with the increment of heating time due to the effect of IMC. The strength of solder bump for each pad is in the range of 9~11N for the heating time over 2sec. The shear strength for Au/Ni/Cu and Au/Cu pads is high at 1.5~2sec and Ni/Cu pad shows the high strength at 2.5~3sec.
2) IMC thickness shows the tendency to increase with the increment of heating time. IMC of Au/Cu pad is thicker than others, as the diffusion rate of solder is better in Cu than Ni. The shear strength decreases with the increment of IMC thickness, therefore, IMC is considered to have an effect on the reliability of the solder bump.
3) Comparing the variation of IMC thickness of solder bumps by induction heating and hot air reflow, IMC thickness increases with the aging time. IMC thickness

by two soldering processes is similar at the initial stage but IMC thickness by hot air reflow is thicker with the increment of aging time than induction heating. After 16 aging days, IMC thickness by induction heating is thicker than hot air reflow and the thickness is about 3.91㎛.

Reference

1. Mingyu Li, Hongbo Xu, Chunqing Wang, Han Sur Bang, Hee Seon Bang, IMC evolution and reliability of lead-free solder bump formed by induction self heat reflow, Electronic Packaging Technology, 2005 6th International Conference on, pp518-523, 2005.
2. Hyun-Hu Park, Joining characteristics of Ball Grid Array(BGA) solder bump by Induction heating, 2004
3. John H. Lau, Solder joint realiability of BGA, CSP, Flip chip, and Fine pitch SMT assemblies, McGRAW-HILL Book
4. John Davis, Peter Simpson, Induction Heating Handbook, McGRAW-HILL Book, 1979
5. Chester A. Tucbury, Basics of Induction heating, Vol.1
6. 정재필, 신영의, 임승수, 무연마이크로 솔더링, 삼성북스, 2005.
7. Yanhong Tian, Chunqing Wang, Xiushan Ge, Peter Liu, Deming Liu, Intermetallic compounds formation at interface between PBGA solder ball and Au/Ni/Cu/BT PCB substrate after laser reflow processes, Material Science and Engineering B95, pp 254-262, 2002.
8. H.L.J. Pang, K.H. Tan, X.Q. Shi. Z.P. Wang. Microstructure and intermetallic growth on the shear fatigue strength of solder joints subjected to thermal cycling aging. Material Science and Engineering, A 307, pp 42-50, 2001.
9. 한현주, 정재필, 하범용, 신영의, 박재용, 강춘식, BGA용 Sn-3.5Ag 볼의 리플로 솔더링 특성, Vol. 19, No.2, pp 39-44, 4. 2001.
10. Jae-Pil Jung, Hyun-Joo Han, Jae-Yong Park, Choon-Sik Kang, Effect of Reflow Variables on the Characteristic of BGA Soldering, Journal of the Micro electronics & Packaging Society, Vol. 6, No. 3. pp 9-18. 1999.
11. 김문일, 문준권, 정재필, Sn-Ag-X계 무연솔더 접합부의 미세조직 및 전단강도에 관한 연구, 대한용접학회지, Vol. 20, No. 2. pp 195-199, 4. 2002.
12. 김경섭, 이석, 김헌희, 윤준호, μBGA 패키지에서 솔더볼의 초기 접합강도와

금 확산에 관한 연구, 대한용접학회지, Vol. 19. No. 3, 6, 2001.
13. 신창근, 정재필, 허주열, BGA 솔더조인트의 전단강도에 미치는 Cu 첨가 솔더의 영향, 마이크로전자패키징학회, Vol.7, No. 2, pp. 13-19. 2000.
14. 신영의, Micro soldering의 프로세스와 그 신뢰성, 대한용접학회지,Vol.13, No. 4, pp. 14-23. 1995.
15. 이재식, 정재필, 김숙환, 솔더링부의 금속학적 특성 및 강도평가, 대한용접학회지, Vol.20, No.4, pp. 31-36. 2002.
16. 신영의, Micro Soldering 의 프로세스와 그 신뢰성, 대한용접학회지, Vol. 13, No.4, pp 14-23, April. 1995.
17. 이창배, 이창열, 서창제, 정승부, 무연솔더 접합계면의 금속간 화합물 생성 및 성장, 대한용접학회지, Vol.20, No.3, pp. 16-22. 2002.
18. 김미진, 김문일, 신규식, 정재필, 전자부품에서의 무연솔더, Micro electronics & Packaging Society, Vol. 7, No. 4. pp 49-56. 2000.
19. 신영의, 이석, 코조후지모토, 김종민, 48μBGA에 적용한 무연솔더의 시효처리에 대한 금속간 화합물의 특성, Micro electronics & Packaging Society, Vol. 8, No. 3. pp 37-42. 2001.
20. 박세훈, 김영호, 무연 솔더 범프의 신뢰도 평가와 솔더 계면 분석에 관한 연구